ISSN : 2249 - 8877 Volume 6 Issue 4

Research & Reviews On Polymer

Full Paper

RRPL, 6(4), 2015 [140-147]

Quasi-three dimensional model of polymer flows in c-shaped chamber for twin-screw extruders with closely intermeshing screws

O.I.Skul'skiy

Ural Department of Russian Academy of Science, Institute of Continuous Media Mechanics, Perm, (RUSSIA)

E-mail: skul@icmm.ru

ABSTRACT

This paper presents same new approaches to model the flow and heat transfer processes in the channels in twin-screw extruders. The nnumerical algorithm based on the finite element method is developed. The fields of the pressure, temperature and velocity in the screw channel are obtained.

KEYWORDS

Twin-screw extruders;
Quasi-three dimensional mathematical model;
Numerical methods.

INTRODUCTION

In the last few years there has been a growing industrial demand for twin-screw extruders, which have some advantages over single screw extruders: (i) the output is pulsation free and only slightly dependent on the properties of extruded materials (ii) the residence time of each material portion in the extruder channels is nearly the same (iii) they are capable of self-cleaning.

Single screw extruders have long been the subject of thorough theoretical analysis based on the well-established analytical and numerical methods. As for twin screw extruders, the problem of mathematical modelling is still acute and requires further consideration. This paper presents some new approaches to model the flow and heat transfer processes in the channels of twin-screw extruders.

An approximate analysis of twin-screw extruders is usually based on the Shenkel theory. According to this theory the capacity of extruder is the total volume of extrusion processed material that becomes free per unit time

$$Q_{\max} = 2mNV, \quad (1)$$

where m a number of thread starts per screw is, N is the rotation rate and V is the C-shaped chamber volume. The net throughput is actually less than the theoretical value by the amount of leakage flow through the gaps

$$Q = Q_{\max} - \Delta Q_p - \Delta Q_c, \quad (2)$$

where ΔQ_p is the net leakage flow due to global pressure drop which is defined by the die resistance, ΔQ_c is the net leakage flow due to the local pressure drops in the gaps. The leakage flows can be calculated when the pressure drops in these gaps are known. All types of the leaks observed during co-rotation and counter-rotation of screws have been discussed elsewhere[1].

A comprehensive analysis of leakage flows for both the Newtonian and power-law liquids is given in the papers by Kim with co-authors[2,3]. Although the analysis has been developed to the level of

analytical formulae, the calculations of some specified variants is rather tedious procedure and demands computer calculations. It is hardly probable that the calculations of velocity and pressure distributions throughout C-shaped chamber could be realized in analytical form, even in the case of isothermal version. In articles[4-9] a few numerical models of flow in twin-screw extruders have been proposed.

Here we present a method of reducing complex three-dimensional problem of the flow and heat transfer in the screw-channels of twin-screw extruders to a quasi-three dimensional problem in an equivalent C- shaped chamber. This statement allows the longitudinal flow and the transverse circulation to be taken into account.

STATEMENT OF THE PROBLEM

The twin-screw extruders are produced of two types: (i) with co-rotating screws having the same helix angles $\varphi_1 = \varphi_2$, and (ii) with counter-rotating screws with helix angles differing in sign $\varphi_1 = -\varphi_2$.

Twin-screw extruders are commonly manufactured with closely intermeshing screws. This results in high pumping effect and pulsation free output. The exception is mixing zones with increased transverse gaps which provide intense material exchange between screws and as a result high quality mixing.

Consider now an inter flight spacing of screw I assuming that the transverse gaps are small enough to ignore the material exchange between the screws and bearing in mind that the portion of the channel is occupied by the flights of screw II (Figure 1).

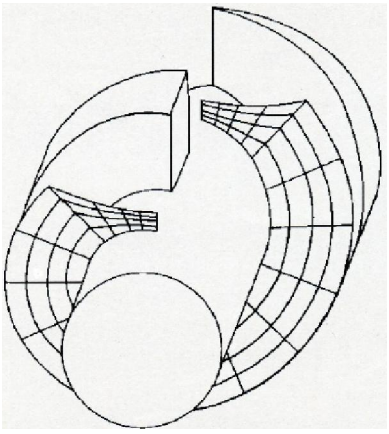

Figure 1 : A C-shaped chamber with calculated section

The spatial figure is formed by a family of helix lines having the following features:

1) The principal normal to a helix line coincides at each point with the normal to the corresponding parent cylinder.
2) The tangents to the helix line form a constant angle with z-axis which is the same as helix angle φ.
3) The helix line of the cylinder has a constant curvature differing from the cylinder radius by a constant multiplier $\rho = R/Cos\varphi$.

To simplify geometry of the design basis we may bring the ends of the C-shaped chamber in coincidence moving them parallel to z-axis while leaving the value and relative directions of boundary velocities unchanged. The resulting unclosed torus has the shape of "bited of bread ring". By all of wing for the helix features, the external radius of torus is set to be equal to the curvature radius of helix line. The inner radius is calculated by assuming that the screw and torus are equal in depth. The width of the torus is equal to the shortest distance between the flanks of the screw flights. In this case the velocity and temperature gradients in the radial and transverse directions match exactly, and in the circumferential direction they well approximate the gradients aligned with the helix lines $\rho = \dfrac{R}{\cos\varphi}$.

Two single vectors coincident with the directions of the principal normal and tangent and the single vector perpendicular to them form the helix coordinate trihedron. The velocity vector components of this system are related to cylindrical coordinates in such a way

$$v_r = v_\rho,\ v_\theta = v_\tau Cos\varphi - v_\varsigma Sin\varphi,\ v_z = v_\tau Sin\varphi + v_\varsigma Cos\varphi . \quad (3)$$

Since it is not essential, whether the rotation is performed by screw or by barrel, it is reasonable to use the inverted motion at which the screw is fixed and the extruder barrel and O_2 axis of screw 2 rotate about the O_1 axis. Hence, the points belonging to screw 1 have zero velocity

$$v_\rho = 0,\ v_\tau = 0,\ v_\varsigma = 0 . \quad (4)$$

and the velocities of the barrel points are

$$v_\rho = 0,\ v_\tau = \omega R Cos\varphi,\ v_\varsigma = \omega R Sin\varphi . \quad (5)$$

Full Paper

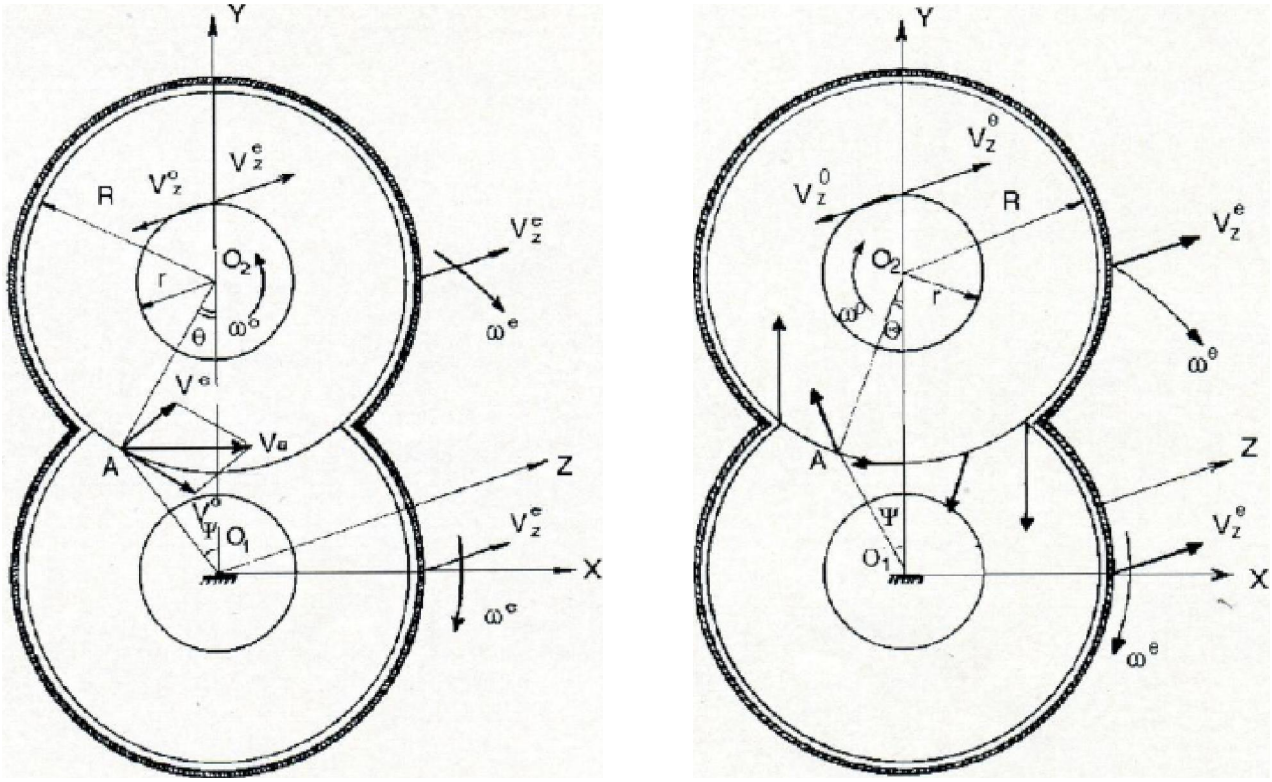

Figure 2 : Scheme to obtain boundary conditions a) co-rotating screws, b) counter-rotating screws)

With the boundary points belonging to screw 2, the situation is more complicated. In this case the velocity components depend on the sense of screw rotation. When the screws are co-rotating, in the inverted motion the resulting velocities of all flight points of screw 2 are seen to be constant and coincident with the x-axis direction (Figure 2a). Assume that the point A belongs to the second screw and is involved in the translational motion with such components as

$$v_\tau^t = \omega\overline{O_1A}Cos\varphi, \quad v_\varsigma^t = \omega RSin\varphi\,. \qquad (6)$$

The length of segments $\overline{O_1A}$ changes with the angle θ according to the following equation

$$\overline{O_1A} = \sqrt{\overline{O_1O_2}^2 - 2R\overline{O_1O_2}Cos\theta + R^2}\,,$$

where $-\dfrac{\overline{O_1O_2}}{2R} \le Cos\theta \le \dfrac{\overline{O_1O_2}}{2R}$. (7)

The relative motion of the point A, has the components

$$v_\tau^t = \omega RCos\varphi, \;\; v_\varsigma^t = \omega RSin\varphi\,. \;(8)$$

Since ς-th components of the translational and relative velocities are equal in modulus but opposite in direction, the resulting velocity $V_\xi^A = 0$. From the similarity of the triangle ΔO_1AE to the triangle formed by vectors $V_\tau^t + V_\tau^r = V^A$, it follows that the algebraic sum of the velocity projections V_τ^t and V_τ^r on the y and z axes is equal to zero, and the V^A ? vector projection on the x axis does not depend on θ and may be expressed as

$$v_x^A = \omega\overline{O_1O_2}Cos\varphi\,. \qquad (9)$$

When the screws are counter-rotating, the translational motion remains as before, and in the relative motion the sign of circumferential velocity changes. The velocity projections of the arbitrary point on the x, y and z-axes take the form

$$\begin{aligned} v_x^A &= \omega\left(2RCos\theta - \overline{O_1O_2}\right)Cos\varphi, \\ v_y^A &= 2\omega RSin\theta Cos\varphi, \\ v_z^A &= 0. \end{aligned} \qquad (10)$$

At $\theta = 0$, the resulting velocity is directed horizontally towards the flow. At the intersection points

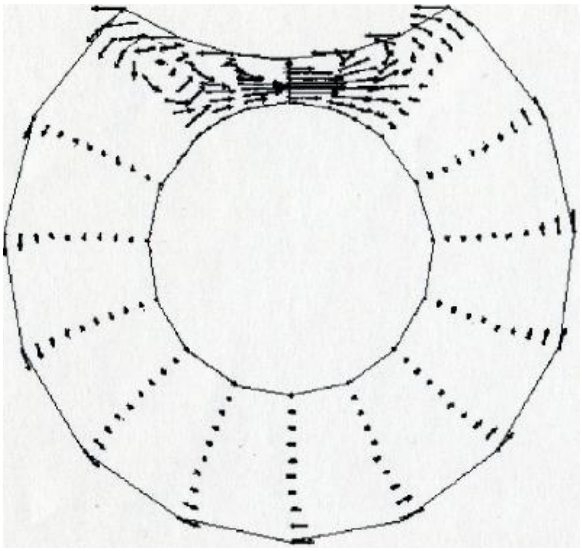

Figure 3 : Velocity vectors of the main flow for co-rotating screws

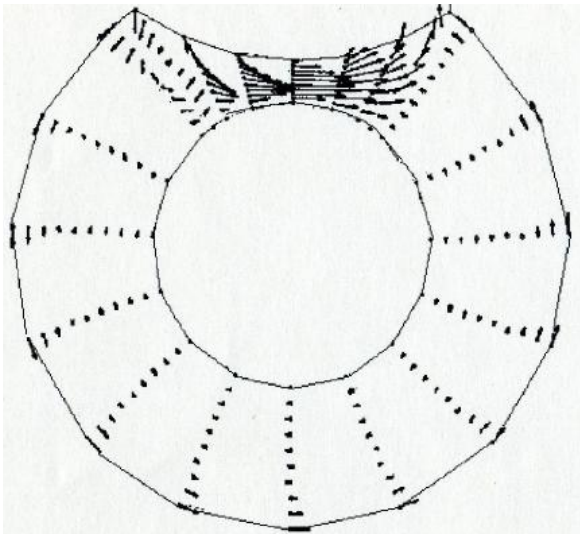

Figure 4 : Velocity vectors of the main flow for counter-rotating screws

of circumferences the horizontal velocity component has become zero and the vertical one is equal to

$$v_y^A = \overline{O_1O_2}\omega Cos\varphi \,. \qquad (11)$$

Figure 3b. shows the velocity vector distribution over screw 2 in terms of moving coordinate system related to screw 1.

For extruder in an operation, the pressure on the inlet cross-section is defined by hydrodynamic resistance of the die. Note however that this pressure is produced only by several last flights. In contrast to the single-screw extruder, the pressure drop in C-shaped chamber of the twin-screw extruder is of local character. The pressure drop at the pumping flights is taken into account by Cauchy equation being prescribed on the radial boundaries of the region

$$\theta = 0 \Rightarrow \boldsymbol{\sigma}\cdot\mathbf{n} = 0,$$
$$\theta = 2\pi \Rightarrow \boldsymbol{\sigma}\cdot\mathbf{n} = -\Delta p. \qquad (12)$$

The boundary conditions (5), (9) or (10) and (12) are sufficient to close the system of differential equations of motion written for the C-shaped chamber.

The output of the twin-screw extruder is defined by the doubled volumetric flow rate through the torus cross-section. The flow rate through the circular cross-section corresponds to the leakages through the gaps between the barrel and flights. Therefore, although the canonical domain becomes simpler, the

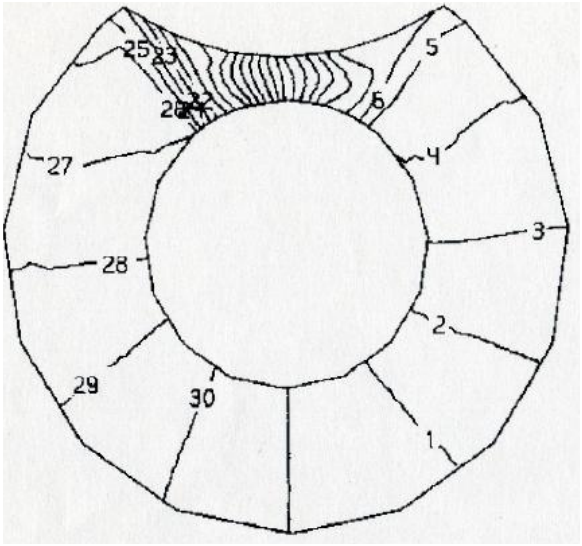

Figure 5 : Isobars for co-rotating screws Pmax=12.0 MPa

problem remains three-dimensional in this formulation. By assuming that all components of the velocity vector are unchanged across the width of the channel we may reduce the problem to two-dimensional one with respect to coordinates while maintaining all three velocity components.

Let us consider the central longitudinal section of the torus. Now the system of differential equations of equilibrium and heat transfer can be represented in cylindrical coordinates assuming that all derivatives along the z-axis normal to the section are zero except $\partial P/\partial z = const$.

$$\rho\left(v_r\frac{\partial v_r}{\partial r}+\frac{v_\theta}{r}\frac{\partial v_r}{\partial\theta}-\frac{v_\theta^2}{r}\right)=-\frac{\partial p}{\partial r}+\frac{\partial}{\partial r}\left(2\eta\frac{\partial v_r}{\partial r}\right)+\frac{2}{r}\eta\frac{\partial v_r}{\partial r}+$$
$$+\frac{1}{r}\frac{\partial}{\partial\theta}\left[\eta\left(\frac{\partial v_\theta}{\partial r}+\frac{1}{r}\frac{\partial v_r}{\partial\theta}-\frac{v_\theta}{r}\right)\right]-\frac{2}{r}\eta\left(\frac{1}{r}\frac{\partial v_\theta}{\partial\theta}+\frac{v_r}{r}\right), \quad (13)$$

$$\rho\left(v_r\frac{\partial v_\theta}{\partial r}+\frac{v_\theta}{r}\frac{\partial v_\theta}{\partial\theta}+\frac{v_r v_\theta}{r}\right)=-\frac{1}{r}\frac{\partial p}{\partial\theta}+\frac{\partial}{\partial r}\left[\eta\left(\frac{\partial v_\theta}{\partial r}+\frac{1}{r}\frac{\partial v_r}{\partial\theta}-\frac{v_\theta}{r}\right)\right]+$$
$$+\frac{2\eta}{r}\left(\frac{\partial v_\theta}{\partial r}+\frac{1}{r}\frac{\partial v_\theta}{\partial\theta}-\frac{v_\theta}{r}\right)+\frac{2}{r}\frac{\partial}{\partial\theta}\left[\eta\left(\frac{1}{r}\frac{\partial v_\theta}{\partial\theta}+\frac{v_\theta}{r}\right)\right], \quad (14)$$

$$\rho\left(v_r\frac{\partial v_z}{\partial r}+\frac{v_\theta}{r}\frac{\partial v_z}{\partial\theta}\right)=-\frac{\partial p}{\partial z}+\frac{\partial}{\partial r}\left(\eta\frac{\partial v_z}{\partial r}\right)+\frac{\eta}{r}\left(\frac{\partial v_z}{\partial r}\right)+\frac{1}{r}\frac{\partial}{\partial\theta}\left[\frac{\eta}{r}\left(\frac{\partial v_z}{\partial\theta}\right)\right], \quad (15)$$

$$\frac{1}{r}\frac{\partial}{\partial r}(rv_r)+\frac{1}{r}\frac{\partial v_\theta}{\partial\theta}=0, \quad (16)$$

$$\rho C_p\left(v_r\frac{\partial T}{\partial r}+\frac{v_\theta}{r}\frac{\partial T}{\partial\theta}\right)=\frac{\partial}{\partial r}\left(\lambda\frac{\partial T}{\partial r}\right)+\frac{1}{r}\lambda\frac{\partial T}{\partial r}+\frac{1}{r^2}\frac{\partial}{\partial\theta}\left(\lambda\frac{\partial T}{\partial\theta}\right)+\Phi. \quad (17)$$

Furthermore, the transverse component v_z must satisfy the following conditions

$$\int_{R_0}^{F(\theta)} v_z dr = Q_f \text{ , in intermeshing zone,} \quad (18)$$

$$\int_{R_0}^{R_1} v_z dr = Q_\delta \text{ , outside intermeshing zone,} \quad (19)$$

which corresponds to prescribing the leakage flow through the gaps between the barrel and the flights Q_δ and between the flights of intermeshing screws Q_f.

Substituting physical equations of, for example, a power-law fluid into the equilibrium equations and integrating by parts, we may reduce the problem to the generalized solution $\{v_r, v_\theta, v_z, p, t\}$, which satisfies the integro-differential equation system

$$w\int_0^{2\pi}\int_{R_0}^{F(\theta)}\left\{\rho u_r\left(v_r\frac{\partial v_r}{\partial r}+\frac{v_\theta}{r}\frac{\partial v_r}{\partial\theta}-\frac{v_\theta^2}{r}\right)-\frac{\partial u_r}{\partial r}p+\eta\left(2\frac{\partial u_r}{\partial r}\frac{\partial v_r}{\partial r}+\frac{1}{r}\frac{\partial u_r}{\partial\theta}\frac{\partial v_r}{\partial\theta}+\right.\right.$$
$$\left.\left.+2\frac{u_r v_r}{r^2}+\frac{1}{r}\frac{\partial u_r}{\partial\theta}\frac{\partial v_\theta}{\partial r}-\frac{1}{r^2}\frac{\partial u}{\partial\theta}v_\theta+2\frac{u_r}{r^2}\frac{\partial v_\theta}{\partial\theta}\right)\right\}rdrd\theta=0, \quad (20)$$

$$w\int_0^{2\pi}\int_{R_0}^{F(\theta)}\left\{\rho u_\theta\left(v_r\frac{\partial v_\theta}{\partial r}+\frac{v_\theta}{r}\frac{\partial v_\theta}{\partial\theta}-\frac{v_\theta v_r}{r}\right)-\frac{1}{r}\frac{\partial u_\theta}{\partial\theta}p+\eta\left(\frac{2}{r^2}\frac{\partial u_\theta}{\partial\theta}\frac{\partial v_\theta}{\partial\theta}+\right.\right.$$
$$+\frac{\partial u_\theta}{\partial r}\frac{\partial v_\theta}{\partial r}-\frac{\partial u_\theta}{\partial r}\frac{v_\theta}{r}-\frac{u_\theta}{r}\frac{\partial v_\theta}{\partial r}+\frac{u_\theta v_\theta}{r^2}+\frac{1}{r}\frac{\partial u_\theta}{\partial r}\frac{\partial v_r}{\partial\theta}$$
$$\left.\left.-\frac{u_\theta}{r^2}\frac{\partial v_r}{\partial\theta}+\frac{2}{r^2}\frac{\partial u_\theta}{\partial\theta}v_r\right)\right\}rdrd\theta=0, \quad (21)$$

$$w\int_0^{2\pi}\int_{R_0}^{F(\theta)}\psi\left\{\frac{1}{r}\frac{\partial}{\partial r}(rv_r)+\frac{1}{r}\frac{\partial v_\theta}{\partial\theta}\right\}rdrd\theta=0, \quad (22)$$

$$w\int_0^{2\pi}\int_{R_0}^{F(\theta)}\left\{\rho u_z\left(v_r\frac{\partial v_z}{\partial r}+\frac{v_\theta}{r}\frac{\partial v_z}{\partial\theta}\right)-\frac{\partial u_z}{\partial z}p+\right.$$
$$\left.\eta\left(\frac{\partial u_z}{\partial r}\frac{\partial v_z}{\partial r}+\frac{1}{r^2}\frac{\partial u_z}{\partial\theta}\frac{\partial v_\theta}{\partial\theta}\right)\right\}rdrd\theta=\int_0^{2\pi}S_z(\theta)\int_{R_0}^{F(\theta)}u_z rdrd\theta, \quad (23)$$

$$w\int_0^{2\pi}\int_{R_0}^{F(\theta)}\left\{\phi\rho C_p\left(v_r\frac{\partial t}{\partial r}+\frac{v_\theta}{r}\frac{\partial t}{\partial\theta}\right)+\lambda\left(\frac{\partial\phi}{\partial r}\frac{\partial t}{\partial r}+\frac{1}{r^2}\frac{\partial\phi}{\partial\theta}\frac{\partial t}{\partial\theta}\right)\right\}rdrd\theta=$$
$$=w\int_0^{2\pi}\int_{R_0}^{F(\theta)}\phi\Phi rdrd\theta+w\int_{R_0}^{R_1}\phi qrdr, \quad (24)$$

$$\int_{-\theta^*}^{\theta^*}\chi(\theta)\int_{R_0}^{F(\theta)}v_z rdrd\theta=Q_f\int_{-\theta^*}^{\theta^*}\chi(\theta)d\theta, \quad (25)$$

$$\int_{\theta^*}^{2\pi-\theta^*}\chi(\theta)\int_{R_0}^{R_1}v_z rdrd\theta=Q_\delta\int_{\theta^*}^{2\pi-\theta^*}\chi(\theta)d\theta, \quad (26)$$

where u_i, H, ψ are functions of coordinates having in variational formulation the meaning of virtual velocities, pressure and temperature. The distributed load S_z has physical meaning of total pressure acting on the screw flight and is unknown value being determined from the system (20-26). To preserve the symmetry, the equation (25, 26) is multiplied by the arbitrary function and integrated with respect to θ.

The system (20-26) is conveniently solved by the finite element method by using a standard procedure. The solution provides the velocity, temperature and pressure fields as well as the integral characteristics of the flow: the throughput and pumping capability of one chamber.

It should be noted that the final scheme was obtained on the basis of more rough but easily realized assumption and allows the tapered screw extruders to be calculated. To solve the problem according to this scheme by the finite element method, we may use a slightly modified algorithm and program developed for the single-screw extruder.

RESULTS

Let us consider now the twin-screw extruder with following parameters: $R_1=100\,mm$ - is the radius of the barrel, $R_0=80\,mm$ - is the screw root radius; $\varphi=14°$ is the angle of the helix line. The calender gap δ may range from 0 to $9\,mm$ and the side clearances between the screw flights are negligibly small and taken to be zero. The temperature of the barrel walls and screw flank is $100°C$, and the inlet temperature of the material is $90°C$. Following mathematical models considered before, the velocity, pressure and temperature distributions were calculated for various values of calender gaps in co-rotating and counter-

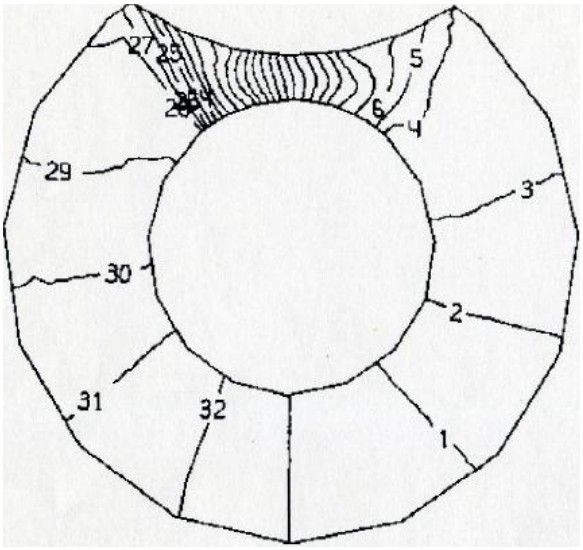

Figure 6. Isobars for counter-rotating screws Pmax=12.8 MPa

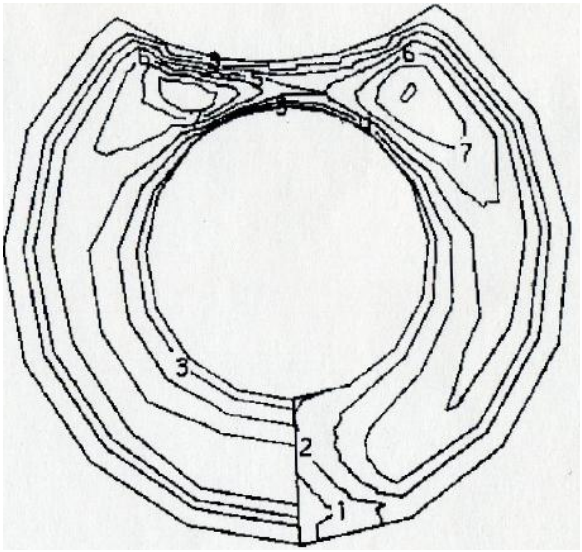

Figure 7 : Isotherms for co-rotating screws, Tmax=112.0 ºC

rotating screws. Numerical results obtained on the basis of these models agree fairly well (Figure 6-10). For the same gap $\delta = 9\,mm$ and with the same rotational speed $\omega = 10\ rpm$ the results calculated by both models differ by less than $10\,\%$. The limited pumping capability in co- rotating screw is higher than in counter-rotating screw.

Narrowing of the gap δ results in the increased pumping capability and more non-uniform temperature field (in zone of calender gap the temperature increases whereas in the rest part it remains practically constant).

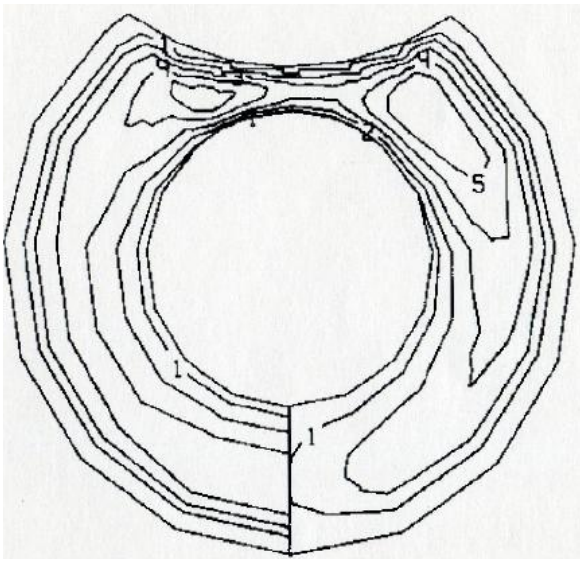

Figure 8 : Isotherms for counter-rotating screws, Tmax =110.5 ºC

CONCLUSION

It is clear from the above discussion that the proposed models of twin screw extruders are in capable of taking into account three-dimensionality of real material flows in the screw channels and all leakages through the gaps, which in fact are not too small to be neglected.

Our models provide data on the processes of flow and heat-transfer in the middle cross-section of C-shaped chamber and calender gap only. However, combined with known two-dimensional models, which consider the cross-section of C-shaped channel well apart from the intermeshing zone, and with the models describing the leakage flows in longitudinal and side gaps they may be effectively used to obtain more complete information on the velocity, pressure and temperature fields in the channels of twin screw extruders.

REFERENCES

[1] L.P.Janssen; Twin screw extrusion, Elsevier Scientific Publishing Company, Amsterdam-Oxford-New York, **(1978)**.

[2] W.S.Kim, W.W.Skatschkow, S.D.Jewmenow; Experimentelle untersuchung des mischprozesses polymerer werkstoffe im doppelschneckenextruder, Plaste und Kautschuk, **22, 9**, 730-734 **(1975)**.

[3] K.T.Nguyen, J.T.Lindt; Finite element modeling of a counter-rotating, non-intermeshing twin screw extruder, Polym.Eng.and Science, **29, 11**, 709-714 **(1989)**.

[4] M.H.Hong, J.L.White; Simulation of flow in an intermeshing modular counterrotating twin screw extruder: Non-Newtonian and non-isothermal behavior, Int'l Polym.Process., **2**, 136–143 **(1999)**.

[5] O.S.Carneiro, G.Caldeira, J.A.Covas; Flow patterns in twin-screw extruders, Journal of Materials Processing Technology, **92-93**, 309-315 **(1999)**.

[6] D.Goffart, D.J.Van Der Wal, E.M.Klomp, H.W.Hoogstraten, L.P.B.M.Janssen, L.Breysse, Y.Trolez; Three-dimensional flow modeling of a self-wiping corotating twin-screw extruder, Part I: The Transporting Section // Polymer engineering and science, **36, 7**, 901-911 **(1996)**.

[7] S.Bakalis, M.V.Karwe; Velocity distributions and volume flow rates in the nip and translational regions of a co-rotating, Self-wiping, twin-screw extruder, Int.J.Food Sci.Technol., **51**, 273–82 **(2002)**.

[8] P.A.McGuire, S.Blackburn, E.M.Holt; Twin-screw extrusion modelling, Advances in science and technology, **45**, 436-441 **(2006)**.

[9] M.H.Hong, Q.Jiang, J.L.White; Experimental studies on screw characteristics in closely intermeshing counter-rotating twin screw extruder, Int'l Polym.Process., **1**, 88–92 **(2008)**.